Complexation of Flavonoids with Iron: Structure and Optical Signatures

Jun Ren,[†] Sheng Meng,[†] Ch. E. Lekka,[‡] and Efthimios Kaxiras*[,†]

Department of Physics and School of Engineering and Applied Sciences, Harvard University, Cambridge, Massachusetts 02138, and Department of Materials Science and Engineering, University of Ioannina, Ioannina 45110, Greece

Received: August 28, 2007; In Final Form: October 31, 2007

Flavonoids exhibit antioxidant behavior believed to be related to their metal ion chelation ability. We investigate the complexation mechanism of several flavonoids, quercetin, luteolin, galangin, kaempferol, and chrysin, with iron, the most abundant type of metal ions in the body, through first-principles electronic structure calculations based on density functional theory (DFT). We find that the most likely chelation site for Fe is the 3-hydroxyl-4-carbonyl group, followed by 4-carbonyl-5-hydroxyl group and the 3′-4′ hydroxyl (if present) for all of the flavonoid molecules studied. Three quercetin molecules are required to saturate the bonds of a single Fe ion by forming six orthogonal Fe−O bonds, though the binding energy per molecule is highest for complexes consisting of two quercetin molecules and one Fe atom, in agreement with experiment. Optical absorption spectra calculated with time-dependent DFT serve as signatures to identify various complexes. For the iron-quercetin complexes, we find a redshift of the first absorbance peak upon complexation in good agreement with experiment; this behavior is explained by the narrowing of the optical gap of quercetin because of Fe(d)−O(p) orbital hybridization.

1. Introduction

Flavonoids are the most abundant polyphenolic compounds found in higher vascular plants, particularly in the leaves, fruits, nuts, skins, flowers, and plant extracts such as red wine and tea.[1] There have been numerous investigations of flavonoids in recent years because of their beneficial pharmacological properties, such as antitumor, antibacterial, and antimutagenic activity and cardiovascular protection.[2−4] In addition, their antioxidant activity is important in prevention and treatment of oxidation damage.[5−7] For example, quercetin (Que), a typical dietary flavonol subclass of flavonoids, has attracted attention because of its high radical-scavenging activity established by experiments.[8−10] It has the ability to chelate metal ions, which is believed to be related to its strong antioxidant behavior and DNA protection.[11,12]

Of all metals in the body, iron is the most abundant; excessive concentration of iron ions may be problematic, leading to production of free hydroxyl radicals through the Fenton reaction.[13,14] The interaction between Fe ions and flavonoids is of crucial importance: flavonoids can scavenge Fe ions through charge transfer from its deprotonated hydroxyl group to form phenoxyl radicals. As a result, flavonoids efficiently bind iron ions and prevent the Fenton reaction from occurring, thus, providing protection from oxidative damage.[11,12] Several investigations have emphasized that the biochemical activity of flavonoid complexes depends strongly on the relative position of the OH groups on the different rings[6] and the metal ion chelation sites.[15−17] Despite extensive efforts, the atomic structure of metal−flavonoid complexes and the binding mechanism remain unclear, mainly because of experimental difficulties in detecting these complexes with molecular resolution in solution.[18−20]

In this work, we study the complexation mechanism of several flavonoinds with Fe using first-principles calculations based on density functional theory (DFT). We optimize the structure of the various Fe−flavonoid complexes at different relative concentrations and compare their formation energies. The highest binding energy clearly identifies the 3-hydroxyl-4-carbonyl group as the most probable chelation site for Fe ion, followed by the 4-carbonyl-5-hydroxyl and 3′-4′-hydroxyl groups. These results are relevant to understanding how complexation of flavonoids with iron can lead to protection from oxidation: for example, when the ratio of Fe/Que is 1:2, the complex is the most thermodynamically stable, but it takes a ratio of Fe/Que of 1:3 to fully saturate all of the bonds of Fe and detoxify it. Using time-dependent DFT (TDDFT), we also calculate ultraviolet−visible (UV−vis) spectra for representative complexes as signatures to identify them. We find good agreement with existing experimental data.

2. Computational Methods

The first-principles calculations were carried out with the SIESTA code.[21] We use pseudopotentials of the Troullier-Martins type[22] to model the atomic cores, the Ceperley-Alder form of the local density approximation for the exchange-correlation functional,[23] and a basis of double-ζ polarized orbitals (13 atomic orbitals for C, N, and O, 5 orbitals for H). An auxiliary real space grid equivalent to a plane-wave cutoff of 100 Ry is used. For geometry optimization, a structure is considered fully relaxed when the magnitude of forces on the atoms is smaller than 0.04 eV/Å. For the optical absorbance calculations within TDDFT in the linear response formulation,[24] we use 12 212 steps in time to propagate the wavefunctions with a time step of 1.7×10^{-3} fs, which gives an energy resolution of 0.1 eV. The perturbing external electric field is 0.05−0.1 V/Å, depending on the complex. This computational scheme gives optical absorption spectra that are in good

* Corresponding author.
[†] Harvard University.
[‡] University of Ioannina.

10.1021/jp076881e CCC: $40.75 © 2008 American Chemical Society
Published on Web 01/23/2008

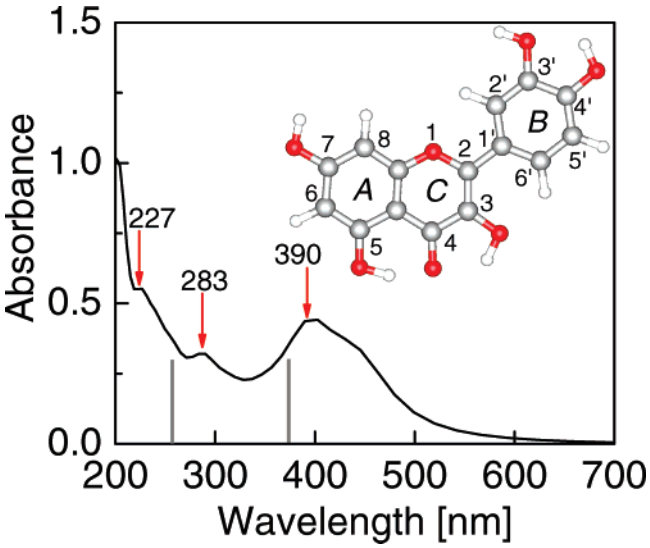

Figure 1. Geometry of a single quercetin molecule (inset: with C, H, and O atoms shown as gray, white, and red spheres) and the corresponding UV−vis spectrum calculated from TDDFT. The two vertical gray lines represent the peak positions and amplitudes in the experimental spectrum.

agreement with experiment for a range of biologically relevant molecules such as DNA bases.[25] All calculations are performed in vacuum and for neutral Fe−flavonoid complexes only; these restrictions, however, do not imply that the flavonoid molecules and Fe atoms are in the neutral state before the reaction that forms the complex. Indeed, the calculations reported here can provide useful insight for complexes obtained from reactions between charged components and for solvated complexes, as we explain in the following sections.

3. Structural Properties of Complexes

We have studied several flavonoid molecules and their respective complexation properties with iron, including quercetin, luteolin (Lut), kaempferol (Kae), galangin (Gal), and chrysin (Chr). A flavonoid molecule in general is composed of two aromatic rings (*A* and *B*) and an oxygenated heterocyclic ring (*C*), as shown in Figure 1 (inset) for quercetin, the 3,5,7,3′,4′-pentahydroxyflavonol. Other flavonoids only differ in the number and sites of OH groups they contain. For instance, luteolin has four OH at the 5,7,3′,4′ sites; kaempferol has OH at the 3,5,7,4′ sites; galangin has OH at the 3,5,7 sites; and chrysin has the smallest number of OH groups, two only, at the 5 and 7 sites. We select these flavonoids to study, because they show very different ion chelation abilities in experiment, related to the number and specific sites of OH groups in their molecular structure.

We will analyze in detail the structure and properties of quercetin, which has the largest number of OH groups, and thus has the highest degree of variability in terms of complexation with metals. For the other flavonoids considered here, we will mostly point out the differences and similarities with quercetin. In the geometry of quercetin obtained from structural optimization, the hydrogen atoms in the hydroxyl groups at positions 3, 5, and 4′ are arranged so as to allow for hydrogen bond formation to the nearby O atoms (of the doubly bonded O at position 4, and of the hydroxyl group at position 3′). The calculated bond length between C4═O4 is 1.279 Å [1.267 Å], between C10−C4 is 1.419 Å [1.418 Å], and between C2−C1′ is 1.456 Å [1.479 Å]; these are all in good agreement with the corresponding experimental values[26] given in square brackets.

In considering the complexation mechanisms, we need to account for changes in the flavonoid structures involving the removal of H atoms from OH units to which the Fe atom is bonded. To this end, we must define the relevant chemical potential for the removed H atoms, the energy of which must be calculated within the same formalism as all other energy values for a meaningful comparison.[27] We considered two choices for the relevant chemical potentials: The first H reservoir corresponds to H_2 molecules and the second to H_2O molecules. Specifically, when H atoms are removed from a flavonoid molecule, they become part of a H_2 molecule for the first reservoir choice, with an energy gain of 2.34 eV per H atom, which is half of the binding energy of the H_2 molecule from our calculation. For this choice of reservoir, the binding energy of the complex is defined as

$$E_b = E_{total} - n_{Fe}E_{Fe} - n_{Que}E_{Que} + n_H E_H + n_H \frac{1}{2} E_{H_2} \quad (1)$$

where E_{total} is the total energy of the complex and E_X, n_X, are the energy and number of species X involved in the complexation reaction (X = Fe, Que, H); in particular, n_H is the number of H atoms missing from the neutral Que molecules after complexation, and E_{H_2} is the binding energy per H_2 molecule. For the second reservoir, the removed H atoms become part of a H_2O molecule; in this case, we take the energy of an isolated H plus half of the H· and ·OH recombination energy (6.07 eV) as the reference for the removed H atoms, which gives an energy gain of 3.04 eV per H atom. By analogy to the first choice of reservoir, the binding energy of the complex with this second reservoir choice is defined as

$$E_b' = E_{total} - n_{Fe}E_{Fe} - n_{Que}E_{Que} + n_H E_H + n_H \frac{1}{2}(E_{H_2O} - E_H - E_{OH}) \quad (2)$$

with similar definitions of symbols as in eq 1. Although somewhat oversimplified, these two choices correspond approximately to the limiting cases of acidic and basic solutions, respectively. Neither choice should be taken literally as corresponding to a true binding energy; instead, the H chemical potential in real physical systems will lie in between the two extremes, depending on the solvent conditions such as pH values. Thus, the two choices of H reservoir give a range of reasonable values for the true binding energy. Actually, depending on the value of the chemical potential within this range, different orderings of the flavonoid complexes in terms of their binding energy can be obtained, as discussed in more detail below.

For consistency and simplicity, we use throughout this work the neutral cluster model for Fe−flavonoid complexes. This does not necessarily imply that the Fe element in the complexes is neutral. In fact, as deprotonation processes take place during Fe−flavonoid complexation with H^+ ions released, the flavonoid molecules are negatively charged and the net charge on Fe−flavonoind complexes may be zero. For example, a neutral complex with one iron and two quercetin molecules, Fe-2Que, can be thought of as the result of removing two H^+, one from each Que molecule which then possesses a negative charge, and combining these two charged Que molecules with one Fe(II) ion to maintain the charge neutrality of the complex. Similarly, there is an Fe(III) ion involved in the Fe-3Que complex and an Fe(I) ion involved in the Fe-Que complex. Using explicitly the charged components as reference states before the reaction would not be a useful comparison for several reasons: First,

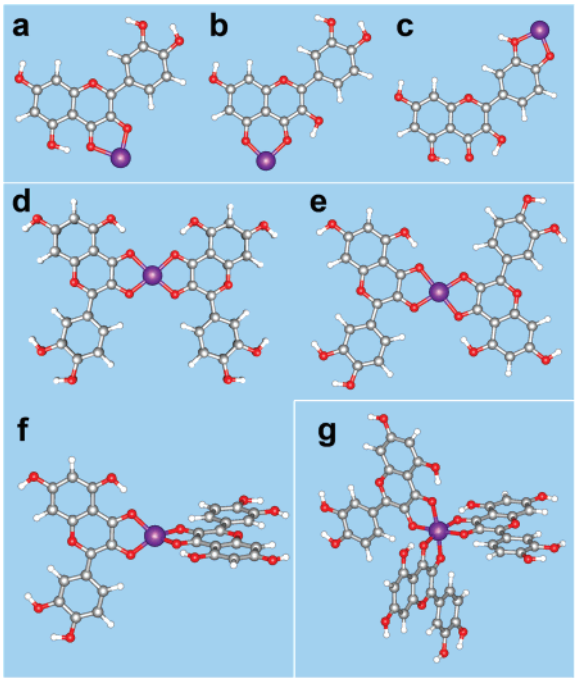

Figure 2. Configurations of different Fe and quercetin complexes. (a) Fe-Que with Fe at the 3-4 site; (b) Fe-Que with Fe (shown as a purple sphere) at the 4-5 site; (c) Fe-Que with Fe at the $3'_H$-4′ site; (d) Fe-2Que in P_R, a planar structure with reflection symmetry; (e) Fe-2Que in P_I, a planar structure with inversion symmetry; (f) Fe-2Que in *O*, a structure with the two molecules on orthogonal planes; (g) Fe-3Que with Fe having six covalent bonds. In d−g, the Fe atom is at the 3-4 site of each molecule.

since solvated molecules are the most interesting for realistic comparison to experiments, the charged states in solution could be strongly screened by hydration shells or neutralized by counterions. Second, DFT calculations are problematic when dealing with systems with large charge, for which energy and structural parameters are less accurate than those for neutral systems. Third, even if we had considered charged systems, charge localization cannot be strictly enforced in DFT calculations, and the excess charge most probably is distributed over several atoms of the complex, making the identification of charged components in the complex impossible. The neutral system adopted here provides a natural, simple, and consistent way to describe the relative stability of iron−flavonoid complexes, especially when trying to implicitly account for possible solvent effects.

Mass spectrometry experiments revealed a number of possible stoichiometries for iron−flavonoid complexes ranging from 1:1 to 1:3.[28] We considered all of these complexes with different relative iron−flavonoid concentrations. For a single flavonoid molecule, there are several possible sites that could bind an iron atom. We classify the chelation sites by the binding energy calculated using the first choice of reservoir for the removed H atoms (H_2 molecules) and discuss implications for using the second choice below. The most favorable ones are shown in Figure 2a−c for quercetin. The corresponding binding energy is 2.09, 1.87, and 1.64 eV per complex (see Table 1, E_b), respectively, relative to a free iron atom, a free quercetin molecule using our first choice of reservoir (H_2 molecules) for the removed H atoms. These results indicate that the preferred site for Fe chelation is the 3-hydroxyl and 4-carbonyl group (denoted as the 3-4 site in the following; the same simplification applies to other cases). The attachment of the Fe atom to the molecule breaks the double bond of the 4-carbonyl group and deprotonates the 3-hydroxyl group to form the two Fe−O bonds.

TABLE 1: Energies and Structural Parameters for Different Fe−Flavonoid Complexes[a]

complex	site	E_b (eV)	E'_b (eV)	*N*	*d* (Å)
Fe-Que	3-4	2.086	2.785	2	1.99
	4-5	1.870	2.569	2	1.95
	$3'_H$-4′	1.639	2.338	2	2.01
	3′-$4'_H$	1.624	2.323	2	2.02
	3′-4′	1.426	2.823*	2	1.90
	3′	1.364	2.063	1	1.80
	4′	1.367	2.066	1	1.81
	7	1.265	1.964	1	1.77
Fe_2-Que	3-4;$3'_H$-4′	3.585	4.982	4	2.00
	3-4;3′-$4'_H$	3.546	4.943	4	2.01
	3-4;3′-4′	3.370	5.466*	4	1.91
Fe-Lut	4-5	1.873	2.572	2	1.92
	$3'_H$-4′	1.667	2.366	2	2.02
	7	1.324	2.023	1	1.79
	3′-4′	1.191	2.588*	2	1.85
Fe_2-Lut	4-5;$3'_H$-4′	3.495	4.892	4	1.96
Fe-Kae	3-4	2.093	2.792	2	2.00
	4-5	1.877	2.576	2	1.96
	7	1.326	2.025	1	1.80
	4′	1.323	2.022	1	1.80
Fe-Gal	3-4	2.056	2.755	2	2.01
	4-5	1.842	2.541	2	1.93
	7	1.316	2.015	1	1.79
Fe-Chr	4-5	1.880	2.579	2	1.93
	7	1.290	1.989	1	1.80

[a] Iron binding energy (E_b and E'_b, with respect to different reservoir choice for the removed H atoms, see text), number of Fe−O bonds (*N*), and average Fe−O bond length (*d*) are listed. H atoms are removed from the OH binding sites unless denoted with a subscript H. The cases in which the choice of reservoir makes a difference in the ordering of the binding energy are marked by an asterisk.

The next site is the 4-carbonyl-5-hydroxyl group (denoted as the 4-5 site). Fe chelation at the 4-5 site is not only thermodynamically less stable, but also less likely because of kinetics: deprotonation of the 5-OH group requires 0.5 eV more energy than deprotonation of the 3-OH group. After Fe binding at 3-4, deprotonation of the 4-5 site cannot bind another Fe because of steric repulsion.

The next available site is the 3′-4′ site. Here, either one or both H atoms can be removed from the 3′- and 4′-hydroxyls, denoted as $3'_H$-4′, 3′-$4'_H$, 3′-4′ sites, respectively, in Table 1. The subscript H represents H atoms not removed from the corresponding site, for instance, Fe binding at the $3'_H$-4′ site is shown in Figure 2c. Leopoldini et al.[17] calculated several Fe(II)-Que complexes and found that Fe binding at 3′-4′ site is 0.5−1.0 eV less stable than binding at the 3-4 and 4-5 sites, with the 3-4 site being the most stable after the complex is hydrated by 2-4 water molecules. Our results also suggest that binding at the 3-4 site is stronger than at the 3′-4′ site: for complexes containing one Fe, the Fe-Que binding strength at different sites has the order 3-4 > 4-5 > 3′-4′, while for complexes containing two Fe atoms, the complex with one Fe bound at the 3-4 site and the second Fe at the 3′-4′site has a binding energy (3.4−3.6 eV**)** which is considerably smaller than twice the binding energy of the one-Fe complex with Fe bound at the 3-4 site ($2 \times 2.1 = 4.2$ eV). However, we note that using the second choice of reservoir for the removed H atoms could result in different ordering in binding energy. The binding energy calculated by using H_2O as the H reservoir is also listed in Table 1 (E'_b). The biggest change using this choice of reservoir is that the 3′-4′ site with two H atoms removed now becomes slightly more favorable than the 3-4 site. The three cases where this happens are marked by an asterisk in Table 1. The ordering in binding energy and the relative stability of

complexes remain unchanged, when the same number of removed H atoms is involved.

Other possible chelation sites, such as the 7-hydroxyl, have a lower binding energy ~1.3 eV per complex. The 1-oxygen and 4-carbonyl have much lower binding energies (<0.4 eV) and will not not be considered further. Experimental measurements of ^{1}H nuclear magnetic resonance (NMR) spectra[18] show that the signal for the proton of the 3-OH group disappears after the Fe-Que complex is formed, which confirms the importance of the 3-hydroxyl-4-carbonyl site (Figure 2a) as the preferred site for Fe chelation. This is consistent with our calculations which give the largest binding energy and a lower deprotonation barrier for this site, with the first choice of reservoir for removed H atoms.

Interestingly, the preference of the 3′-4′ site over the 3-4 site at lower H chemical potential reconciles the current contradiction in the literature about Fe chelation sites: Some studies report that the 3′-4′ site is the first chelation site.[29] This must be due to different solvent conditions (acidic or basic), according to our calculations. Water molecules and other solvent molecules could have a strong influence on the complex structure and stability,[17] but most likely their contribution will be averaged out for complexes of the same size because of thermal fluctuations.

The same trends apply for complexation of other flavonoids (Lut, Kae, Gal, and Chr) with Fe. Our results show that, for all flavonoids investigated, the Fe binding energies are around 2.06−2.09 eV for the 3-4 site, and 1.84−1.88 eV for the 4-5 site, 1.6 eV for the 3′$_H$-4′ site or the 3′-4′$_H$ (with one H remaining on the 3′ or 4′ hydroxyl sites), and less than 1.3 eV for other sites, using the first H reservoir. This suggests that there is a universal trend for Fe−flavonoid complexation: the 3-4 site is the most favored site if present; otherwise the 4-5 site also binds Fe strongly, given that the deprotonation barrier would be overcome. Only one of these two sites can bind a Fe because of steric repulsion. The comparison of energy and structural characteristics of these complexes contained in Table 1 leads to the following ordering in Fe chelation ability:

$$\text{Que} > \text{Lut} > \text{Kae} > \text{Gal} > \text{Chr}$$

which agrees with experiments.[6,30,28] Accordingly, when we consider complexes with more than one flavonoid molecule, we will focus on Fe-Que complexes with Fe bound at either the 3-4 or 4-5 sites.

The complexation process can continue at higher quercetin concentration. At the ratio of Fe/Que = 1:2, we considered three highly symmetric structures shown in Figure 2d−f. In the first, the two molecules are coplanar, and there is a reflection symmetry plane perpendicular to the plane of the molecule and passing through the position of the Fe atom; in the second, the two molecules are also coplanar, and there is inversion symmetry in the plane with respect to the position of the Fe atom; in the third, the planes of the two quercetin molecules bound by a single Fe are orthogonal to each other. The three geometries are denoted as P_R, P_I, and O symmetry, respectively. The binding energies for Fe in these three structures, per complex, are 4.69 eV for the P_R structure, 4.72 eV for the P_I structure, and 4.78 eV for the O structure. The difference of binding energy suggests that the spatial symmetry plays a role in the Fe complexation process: the quercetin molecules prefer to be arranged on orthogonal planes. Furthermore, the binding energy in the same structure but with Fe bound at the 4-5 site is smaller by 0.36 eV per complex, indicating that in the complexes containing two quercetin molecules the 3-4 chelation site is again preferred. These results are in general agreement with ref 17: for instance, the orthogonal complex is favored over planar complexes in vacuum. There exist also certain differences between our results and those of ref 17: for instance, the 4-5 site was found to be favorable for Fe chelation in the charged systems, while with water hydration the 3-4 site is again preferred. These differences are attributed to different charge states in the two calculations and to solvent effects, both of which may not be satisfactorily treated within DFT.

We also considered a complex with three quercetin molecules bound to a single Fe atom. The chelation site for all three molecules was chosen to be the 3-4 site, consistent with our results for the complexes containing one- and two-quercetin molecules. In the three-Que complex, the planes of the three molecules are mutually perpendicular, as shown in Figure 2g. In this structure, Fe is bound to the quercetin molecules by six Fe−O bonds in an octahedral configuration. The calculated binding energy of 6.47 eV per complex indicates that this structure is of stability comparable to that of the one- and two-Que complexes. However, the binding strength is the strongest in the two-Que complex, with an energy of 2.39 eV per Que molecule, compared with 2.16 eV per Que here in the three-Que complex, and 2.09 eV in the one-Que complex. The Fe−O binding strength may be modified in the presence of water molecules, but we expect this to be a small change because the Fe−H_2O bond is relatively weaker than the covalent bonds between Fe and O responsible for the binding energies compared here. This is consistent with experimental observations in the mass spectrometry, where metal−flavonoid complexes of stoichiometry 1:2 are usually preferred.[28] We investigated the possibility of a four-Que complex, but for this case, we find that the binding energy falls to a rather low value of 4.58 eV per complex (1.14 eV per Que), making this structure unlikely to occur. From these results, we conclude that the Fe ions are chemically saturated when bound to three quercetin molecules. The high stability of Fe-3Que complex may have important and profound biological significance, as was revealed in a recent study that protection against intracellar DNA damage in the presence of peroxides dies when the Fe/Que ratio is larger than 1:3.[12] We will return to this issue in the next section.

4. Optical and Electronic Properties

In experiment, the optical absorption of the molecules is used to identify changes in their structure, such as complexation with metal atoms. To address this issue, we calculate the optical properties of quercetin and its various complexes with Fe using TDDFT. The free quercetin molecule exhibits two major absorption bands as indicated in Figure 1. The first peak is at 390 nm and the second one at 283 nm. The primary peaks in the measured UV−vis spectra are at 372 and 256 nm.[18,16] Our calculation for the optical absorption of quercetin is in good agreement with the experimental values, as shown in Figure 1.

For the Fe/Que = 1:1 complex, the first absorption bands are red-shifted relative to the free quercetin molecule, as shown in Figure 3: the first two peaks are at 474 and 290 nm. In complexes with more quercetin molecules, the first absorption peak is almost at the same position at 470−480 nm, but the intensity is gradually enhanced with quercetin concentration. In addition, the relative intensity of the shoulder at 410 nm decreases, and the second band at around 300 nm shifts to longer wavelength. These intensity changes can be used to identify different stoichiometries of the Fe-Que complex. The intensity change for peaks at 470 and 410 nm is a result of the fact that the 470 nm peak involves only transitions localized on the Que

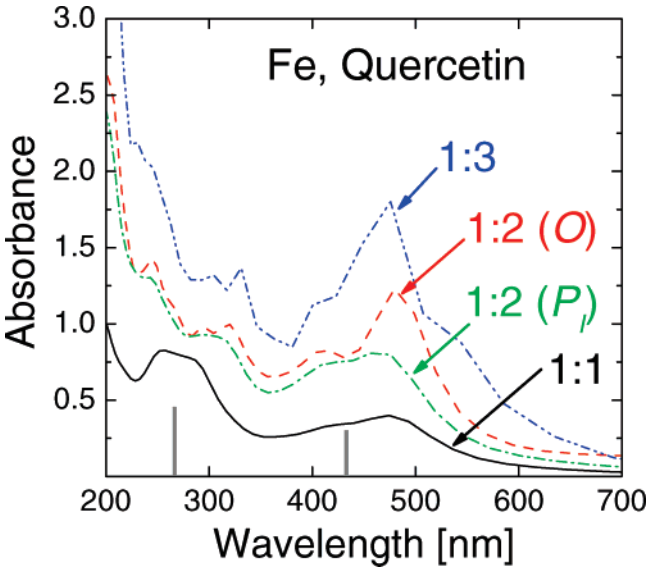

Figure 3. UV−vis spectra of different Fe-quercetin complexes. The ratio of Fe/Que concentration ranges from 1:1 to 1:3. The two vertical gray lines represent experimental peaks. P_I: planar geometry with inversion symmetry. *O*: orthogonal geometry (see text).

molecules while the 410 nm shoulder is due mainly to contributions from the Fe-Que interactions. As a result, the increase of the number of Que molecules in the complex introduces a larger and sharper peak at 470 nm, so that the overall shape of the spectrum for Fe/Que = 1:3 resembles more that of a pure Que molecule, although the first peak has been shifted from 390 to 470 nm. All of the above results are for complexes with Fe bound at the most stable 3-4 site. We have also calculated the complex with Fe at the 3′-4′ site, which gives very similar spectrum as that in Figure 3. In experiments,[18] the corresponding bands of quercetin shift to 430 and 268 nm, respectively, after Fe binding. Although the difference of 40 nm between theory and experiment for the first peak position may appear large, it corresponds to an error of 0.2 eV in the excitation energy, which is within the typical accuracy of TDDFT.[25] Furthermore, the peak in experiment is likely to be a superposition of the peak at 470 nm and the shoulder at 410 nm, because of limited resolution. Most importantly, the general trends in peak positions and intensities upon complexation found through our calculations are in agreement with experimental observations, lending further support to the theoretical analysis presented here.

To elucidate the nature of the absorption peaks and the reasons for their shifts upon complexation, we analyze the electronic structure of the quercetin molecule and its complexes with Fe. The peak at 390 nm in the quercetin absorption spectrum is attributed to electronic excitations from the highest occupied molecular orbital (HOMO) of quercetin to the lowest unoccupied molecular orbital (LUMO). The wavefunctions of these states are presented in Figure 4. The HOMO and LUMO are primarily composed of linear combinations of $2p_z$ orbitals belonging to the C and O atoms: the HOMO comprises mainly π bonding combinations while in the LUMO the antibonding combinations dominate. The HOMO is more localized at the *C* and *B* rings but the LUMO is delocalized from the *B* ring to the C2−C1′ bond and from the C2−C3 bond of the *C* ring to the C3−C4 and C4═O4 bonds. Therefore, the first absorption band has $\pi \rightarrow \pi^*$ character. The change of wavefunction distribution also indicates that the first band has contributions from both the *B* and *C* rings.

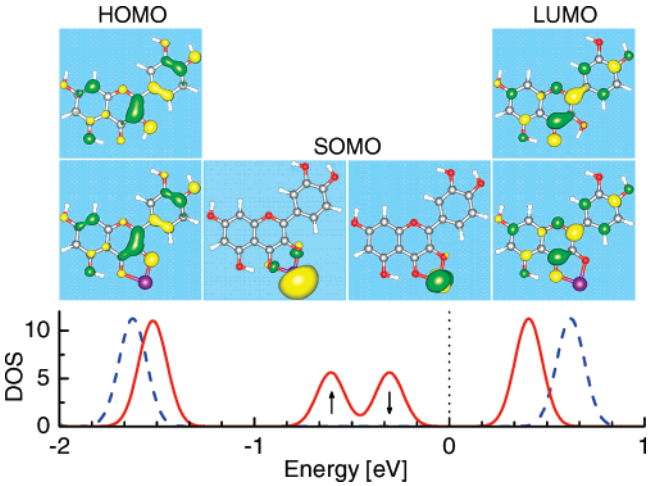

Figure 4. Density of states of the quercetin molecule (dashed line) and the Fe-Que complex (solid line), for the configuration shown in Figure 2a. The upper panels show the corresponding wavefunctions of these orbitals. The dotted vertical line indicates the Fermi level. Arrows indicate the majority (↑) and minority spin component (↓).

Compared to the free quercetin molecule, the HOMO of quercetin in the Fe-Que complex is more delocalized spreading over the C2−C3−C4 atoms, because of the presence of Fe. It is worth noting that the longest wavelength band for the Fe-Que complex is not the transition from the HOMO to the LUMO states of the Que molecule. There exist two singly occupied molecular orbitals (SOMO) between the quercetin-related HOMO and LUMO states (Figure 4). These two states correspond to the 4s orbital of the Fe atom, for the majority spin, and the $3d_{z^2}$ orbital for the minority spin. Consequently, the first absorption band should be around 1920 nm, which corresponds to transitions between the SOMO orbitals related to the bound Fe atom and the LUMO state of the Que complex. However, this band will have very small intensity and will be difficult to detect in experiments. As a result, the first band at ∼430 nm in experimental UV−vis spectra reflects the transition between the HOMO and LUMO states associated with quercetin, as they have been modified by the presence of the Fe atom. Previously, this peak was usually assigned to the ligand-to-metal charge transfer (LMCT) transition;[17] we argue here that it is not the case because the LMCT peak would be at longer wavelength. This is also evidenced by the fact that the three-Que complex shows the same peak though it does not invoke any LMCT peaks as all Fe bonds are saturated. As the position of states shown in Figure 4 makes clear, complexation with Fe moves the HOMO and LUMO states of quercetin closer in energy which accounts for the observed red shift in the first absorption peak discussed earlier.

In contrast to the two SOMO states described above, which are close to the Fermi level, other orbitals of Fe form occupied states located at 3.3−4.2 eV below the Fermi level, as shown in Figure 5. For the majority spin, there is one state at −3.80 eV relative to the Fermi level, with Fe $3d_{xy}$ and $3d_{z^2}$ character and localized at the *A* and *C* rings of the complex; another state at −3.30 eV with $3d_{x^2-y^2}$ and $3d_{z^2}$ character is localized on the *B* and *C* rings. For the minority spin, one state at −4.21 eV has $3d_{x^2-y^2}$ and $3d_{xy}$ character and is localized in the *A* and *C* rings while another at −3.62 eV has $3d_{x^2-y^2}$ and $3d_{z^2}$ character and is localized on the *B* and *C* rings. These states contribute to the transitions around 300 nm in the absorbance spectra of the complexes (see Figure 3). We also found that, for the Fe-2Que complex, only one SOMO state exists between the HOMO and LUMO and that no such state exists for the Fe-3Que complex,

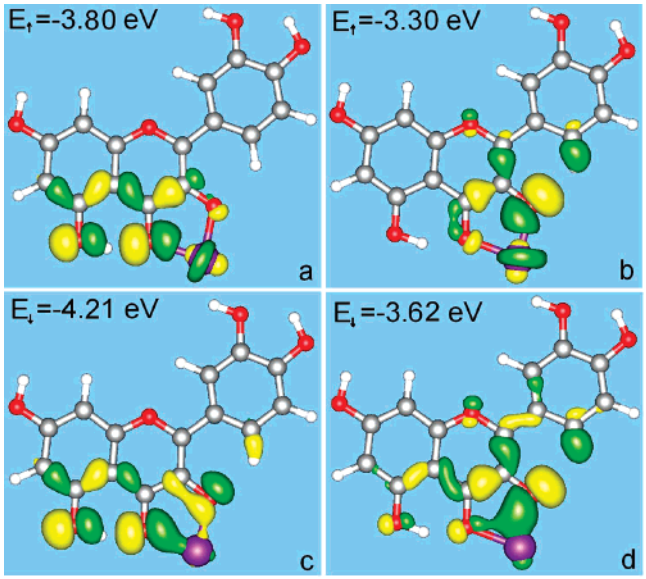

Figure 5. Wavefunctions for the bound states of Fe in the Fe-Que complex shown in Figure 2a and their energies relative to the Fermi level: a and b show the majority spin states; c and d show the minority spin states.

indicating all Fe orbitals are saturated, consistent with our earlier statement that it takes three quercetin molecules to fully saturate the Fe.

5. Conclusions

We have investigated the optimized structure of several Fe−flavonoid complexes and the UV−vis optical spectra of Fe−quercetin complexes containing one Fe atom and one to three quercetin molecules. The highest binding energy for the Fe atom to a single quercetin molecule demonstrates that the 3-hydroxyl-4-carbonyl group is the optimal chelation site, followed by the 4-5, 3′-4′ sites. This is a general trend that applies to all other flavonoids studied here. Furthermore, a complex of two quercetin molecules with a single Fe ion is energetically more stable than complexes with one or three quercetin molecules, but only in the three-quercetin complex are all the orbitals of the Fe atom saturated by formation of covalent bonds. The former is confirmed by experimental observation that Fe/Que = 1:2 complexes are dominant in mass spectrometry. In the one- and two-quercetin complexes with Fe, there exist singly occupied Fe-related states in the original gap between HOMO−LUMO states of Que, but these states disappear in the Fe-3Que complex, indicating that this complex is chemically inert. Our calculated absorbance bands are in good agreement with the experimental data. In particular, the first absorption band for the free quercetin as well as for the Fe−*n*Que (n = 1,2,3) complexes is due to HOMO−LUMO $\pi \rightarrow \pi^*$ transitions in quercetin, and the peak position changes due to energy shifts of these states upon complexation, rather than LMCT. These results form the basis for understanding the structural and electronic properties of Fe−flavonoid complexes and hence their ability to act as antioxidants.

Acknowledgment. We thank D. Galaris, G. Evangelakis, and G. Zonios for introducing us to the problem and for useful discussions.

References and Notes

(1) Herrmann, K. *J. Food Tech.* **1976**, *11*, 433.
(2) Brandi, M. L. *Bone Mineral* **1992**, *19*, S3.
(3) Middleton, E. Kandaswami, C. *Biochem. Pharmacol.* **1992**, *43*, 1167.
(4) Havsteen, B. H. *Pharmacol. Therapeut.* **2002**, *96*, 67.
(5) Husain, S. R.; Cillard, J.; Cillard, P. *Photochemistry* **1987**, *26*, 2489.
(6) Jovanovic, S. V.; Steenken, S.; Tosic, M.; Marjanovic, B.; Simic, M. G. *J. Am. Chem. Soc.* **1994**, *116*, 4846.
(7) van Acker, S. A. B. E.; van Balen, G. P.; van den Berg, D. J.; Bast, A.; van der Vijgh, W. J. F. *Biochem. Pharmacol.* **1998**, *56*, 935.
(8) Robak, J.; Gryglewski, R. J. *Biochem. Pharmacol.* **1988**, *37*, 837.
(9) Bors, W.; Heller, W.; Michel, C.; Saran, M. *Methods Enzymol.* **1990**, *186*, 343.
(10) Ioku, K.; Tsushida, T.; Takei, Y.; Nakatani, N.; Terao, J. *Biochim. Biophys. Acta Biomembr.* **1995**, *1234*, 99.
(11) Afanas'ev, I. B.; Dorozhko, A. I.; Brodskii, A. V.; Kostyuk, V. A.; Potapovitch, A. I. *Biochem. Pharmacol.* **1989**, *38*, 1763.
(12) Melidou, M.; Riganakos, K.; Galaris, D. *Free Radical Biol. Med.* **2005**, *39*, 1591.
(13) Fenton, H. J. H. *J. Chem. Soc.* **1894**, *65*, 889.
(14) Haber, F.; Weiss, J. J. *Proc. R. Soc. London, Ser. A* **1934**, *147*, 332.
(15) Torreggiani, A.; Trinchero, A.; Tamba, M.; Taddei, P. *J. Raman Spectrosc.* **2005**, *36*, 380.
(16) Cornard, J. P.; Merlin, J. C. *J. Inorg. Biochem.* **2002**, *92*, 19.
(17) Leopoldini, M.; Russo, N.; Chiodo, S.; Toscano, M. *J. Agric. Food Chem.* **2006**, *54*, 6343.
(18) de Souza, R. F. V.; Sussuchi, E. M.; De Giovani, W. F. *Synth. React. Inorg. Met.-Org. Chem.* **2003**, *33*, 1125.
(19) Zhou, J.; Wang, L. F.; Wang, J. Y.; Tang, N. *J. Inorg. Biochem.* **2001**, *83*, 41.
(20) Cornard, J. P.; Dangleterre, L.; Lapouge, C. *J. Phys. Chem. A* **2005**, *109*, 10044.
(21) Soler, J. M.; Artacho, E.; Gale, J. D.; García, A.; Junquera, J.; Ordejón, P.; Sánchez-Portal, D. *J. Phys: Condens. Matter* **2002**, *14*, 2745.
(22) Troullier, N.; Martins, J. L. *Phys. Rev. B* **1991**, *43*, 1993.
(23) Ceperley, D. M.; Alder, B. J. *Phys. Rev. Lett.* **1980**, *45*, 566.
(24) Tsolakidis, A.; Sánchez-Portal, D.; Martin, R. M. *Phys. Rev. B* **2002**, *66*, 235416.
(25) Tsolakidis, A.; Kaxiras, E. *J. Phys. Chem. A* **2005**, *109*, 2373.
(26) Rossi, M.; Rickles, L. F.; Halpin, W. A. *Bioorg. Chem.* **1986**, *14*, 55.
(27) Kaxiras, E.; Bar-Yam, Y.; Joannopoulos, J. D.; Pandey, K. C. *Phys. Rev. B* **1987**, *35*, 9625.
(28) Fernandez, M. T.; Mira, L.; Florencio, M. H.; Jennings, K. R. *J. Inorg. Biochem.* **2002**, *92*, 105.
(29) Engelmann, M. D.; Hutcheson, R.; Cheng, I. F. *J. Agric. Food Chem.* **2005**, *53*, 2953.
(30) Sugihara, N.; Arakawa, T.; Ohnishi, M.; Furuno, K. *Free Radical Biol. Med.* **1999**, *27*, 1313.